BIOINFORMATICS

Vol. 00 no. 00 2010
Pages 1–9

Next-Generation VariationHunter: Combinatorial Algorithms for Transposon Insertion Discovery

Fereydoun Hormozdiari[1], Iman Hajirasouliha[1], Phuong Dao[1], Faraz Hach[1], Deniz Yorukoglu[1], Can Alkan[2], Evan E. Eichler[2], S.Cenk Sahinalp[1]

[1] School of Computing Science, Simon Fraser University, Burnaby, BC, Canada
[2] Department of Genome Sciences, University of Washington, and Howard Hughes Medical Institute, Seattle, WA, USA

Received on XXXXX; revised on XXXXX; accepted on XXXXX

Associate Editor: XXXXXXX

ABSTRACT

Recent years have witnessed an increase in research activity for the detection of structural variants (SVs) and their association to human disease. The advent of next-generation sequencing technologies make it possible to extend the scope of structural variation studies to a point previously unimaginable as exemplified by the 1000 Genomes Project. Although various computational methods have been described for the detection of SVs, no such algorithm is yet fully capable of discovering transposon insertions, a very important class of SVs to the study of human evolution and disease. In this paper we provide a complete and novel formulation to discover both loci and classes of transposons inserted into genomes sequenced with high-throughput sequencing technologies. In addition, we also present "conflict resolution" improvements to our earlier combinatorial SV detection algorithm (VariationHunter) by taking the diploid nature of the human genome into consideration. We test our algorithms with simulated data from the Venter genome (HuRef) and are able to discover $> 85\%$ of transposon insertion events with precision of $> 90\%$. We also demonstrate that our conflict resolution algorithm (denoted as VariationHunter-CR) outperforms current state of the art (such as original VariationHunter, BreakDancer and MoDIL) algorithms when tested on the genome of the Yoruba African individual (NA18507).

Availability: The implementation of algorithm is available at `http://compbio.cs.sfu.ca/strvar.htm`.

Contact: eee@gs.washington.edu; cenk@cs.sfu.ca

1 INTRODUCTION

Human genetic variation can be defined in various size ranges. The smallest type of variation, termed single nucleotide polymorphisms (SNPs), are those at the single basepair level. The International HapMap Project genotyped 270 human individuals for 3.1 million SNPs, and recently the 1000 Genomes Project[1] was initiated to characterize human genetic variation with lower minor allele frequency by sequencing more than 1000 human genomes. More recently, it was shown that structural variation (SV) events significantly contribute to human genome diversity (Tuzun *et al*., 2005; Feuk *et al*., 2006; Korbel *et al*., 2007; Kidd *et al*., 2008). Many structural variants are associated with genetic diseases such as psoriasis (Hollox *et al*., 2008) and Crohn's disease (McCarroll *et al*., 2008), prompting an increased interest in structural variation studies (Tuzun *et al*., 2005; Korbel *et al*., 2007; Lee *et al*., 2008; Bashir *et al*., 2008; Hormozdiari *et al*., 2009; Korbel *et al*., 2009; Chen *et al*., 2009; Lee *et al*., 2009; Sindi *et al*., 2009). Recently it was shown that the SV reconstruction is harder than *de novo* assembly of small genomes and introduced an extensive framework for optimal genome re-sequencing (Du *et al*., 2009). Recently, we developed a set of combinatorial algorithms to detect structural variation using high-throughput sequencing data with improved sensitivity through interrogating the repeat and duplication rich segments of the human genome. In (Hormozdiari *et al*., 2009), the maximum parsimony structural variation (MPSV) discovery problem was introduced. This MPSV problem asks to compute unique mapping for each discordant paired-end read in the reference genome such that total number of implied structural variants (SVs) is minimized. We also previously presented a computational analysis of *read depth* to characterize segmental duplications and predict absolute copy number and content of duplicated genes (Alkan *et al*., 2009). See the review from Medvedev *et al.* (Medvedev *et al*., 2009) for the details and strengths of different structural variation discovery methods.

One type of structural variation excluded from this analysis is the mobile element transposition. Mobile elements, or *transposons*, are repetitive elements in the genome that occupy approximately 44% of the human genome, including Alu, L1, and SVA elements (Mills *et al*., 2007). Most of the transposons are fixed in the human lineage; however, around

[1] http://www.1000genomes.org

0.05% of the transposons are still active, and the copy number and loci of these active transposons vary in the genomes of different individuals. Many studies have demonstrated that the mobile elements contribute to genome evolution and human genetic diversity. An interesting case was shown by Bekpen *el al.* (Bekpen *et al*., 2009): insertions of an Alu element were posited to cause pseudogenization of the IRGM gene at the split of New World and Old World monkey lineages 35-40 million years ago (mya) by disrupting the open reading frame (ORF). A second transposon integration (ERV9) restored the ORF $\sim$24 mya in the common ancestor of apes and humans, demonstrating the first report on a "resurrected" gene. The human IRGM gene plays an important role in the immune system (Bekpen *et al*., 2009) and is associated with Crohn's disease (McCarroll *et al*., 2008). Mobile element transpositions are associated with the expansion of interspersed segmental duplications (Bailey *et al*., 2003) and can promote both the creation of segmental duplication in human genomes (Xing *et al*., 2009) and the alteration of gene transcription by gene-trapping and exonization.

Another aspect that most structural variation algorithms ignore is the diploid nature of the human genome (including VariationHunter, BreakDancer (Chen *et al*., 2009), and GASV (Sindi *et al*., 2009)). Each chromosome has exactly two copies; therefore, all loci in the genome (wlog, except segmental duplications) are represented twice. This means that there can not be more than two structural variants (including the "normal" variant signature observed by "concordant" paired-end mapping (Tuzun *et al*., 2005)) at the same locus. However, due to the mapping artifacts in the repetitive segments of the human genome, most algorithms might call multi-allelic structural variants within overlapping intervals. In fact, the limitation of *two variants per locus* information can be used both to reduce false discovery rates and also genotype structural variants (homozygous vs. hemizygous).

In this paper, we present two extensions/improvements to the combinatorial formulation of our original VariationHunter algorithm (Hormozdiari *et al*., 2009) to detect structural variation using high throughput sequencing technology. The main contributions of this paper are (i) the first mathematically complete formulation and algorithm to identify transposition events (especially mobile element transpositions) and (ii) to remove ambiguity in variation discovery through "conflict resolution" (enforcing at most two variants per locus).

We first show that our method for discovery of mobile element transpositions has high accuracy and precision. In a full scale simulation, we produce short reads from the genome of J. Craig Venter (very similar to what an Illumina platform would produce). Our method is able to find around 85% of the known transposon insertions with a precision of more than 90%. We also demonstrate that our new algorithm (denoted as VariationHunter-CR) has a higher accuracy in comparison to VariationHunter(Hormozdiari *et al*., 2009), BreakDancer(Chen *et al*., 2009) and MoDIL(Lee *et al*., 2009) when tested on a whole-genome shotgun sequence data set generated from the genome of the Yoruba African individual (NA18507) using the Illumina platform.

2 DEFINITIONS AND THE FORMULATION OF TRANSPOSITION EVENTS

In (Tuzun *et al*., 2005; Volik *et al*., 2003), a general framework for detecting structural variation using long paired-end reads was introduced. This framework is based on aligning the paired-end reads to the reference genome and observing the *end-reads* [2] with discordant mapping. The paired-end reads with discordant mapping suggest either *deletion*, *insertion*, or *inversion* events. For example, an inversion event can be deduced when one of the two end-reads of a paired-end read has a different mapping orientation than expected. In the standard library construction of the Illumina platform, in the case of no inversions or duplications, the read that maps to the proximal location is expected to be in the $+$ strand, where its mate should be mapped to a distal location in the $-$ strand. However, if the read pair spans an inversion breakpoint, the mapping orientations of the reads will be observed as either $++$ or $--$ (See the Supplementary Material in (Hormozdiari *et al*., 2009) for a full case study).

As per Hormozdiari *et al.* (2009) , we denote a read pair as pe_i and the distance between the end coordinate of the proximal read and the start coordinate of the distal read as the *GapSize* (i.e. the *insert-size* minus the total length of the reads). An alignment of a read pair to the reference genome is denoted as *concordant* (Tuzun *et al*., 2005) if the distance between the aligned end-reads is in the range $[\Delta_{\min}, \Delta_{\max}]$ and the alignment orientation is $+-$. The range $[\Delta_{\min}, \Delta_{\max}]$ is empirically calculated by analyzing the mapping span size distribution of the read pairs.

The set of discordant paired-end reads is represented as $R = \{pe_1, pe_2, \cdots, pe_n\}$. Each discordant paired-end read pe_i may be mapped to multiple locations in the reference genome. The set of all alignments of pe_i is then defined as $Align(pe_i) = \{a_1pe_i, a_2pe_i, \cdots, a_jpe_i\}$.

Note that each alignment of pe_i to the reference genome (a_jpe_i) is a 5-tuple that represents the map locations of the end-reads and their alignment orientation. More formally,

$$a_jpe_i = ((L_\ell(pe_i), L_r(pe_i)), (R_\ell(pe_i), R_r(pe_i)), or(pe_i))$$

where the pair $(L_\ell(pe_i), L_r(pe_i))$ represents the map location (i.e. both start and end loci) of the left end-read of pe_i, $(R_\ell(pe_i), R_r(pe_i))$ is the mapping location of the right end-read of pe_i, and $or(pe_i)$ represents the map orientation of both ends. Note that $or(pe_i) \in \{+-, ++, --, -+\}$.

In (Hormozdiari *et al*., 2009), a structural variation event (in short, SV) is defined as $SV(t, Pos_L, Pos_R, Ran_{\min}, Ran_{\max})$. SV represents a structural variant of type $t \in \{Ins, Del, Inv\}$[3] located between Pos_L and Pos_R in the reference genome, and with size estimated between $Ran_{\min}$ and $Ran_{\max}$.

Another important type of structural variation is the *transposition* event *where a segment of the genome (formally, a transposon) is copied to another location with a small divergence*. In the remainder of this paper we call such types of structural variants as *copy events*. Examples of common copy events include transpositions of Alu, SVA and L1 elements.

[2] The two ends of a read pair is referred as end-reads.

[3] Referring to an insertion, deletion, and inversion event respectively.

Unfortunately, none of the available methods designed to detect structural variation events (e.g. (Tuzun *et al.*, 2005; Korbel *et al.*, 2007; Kidd *et al.*, 2008; Bashir *et al.*, 2008; Lee *et al.*, 2008, 2009; Hormozdiari *et al.*, 2009; Chen *et al.*, 2009; Sindi *et al.*, 2009)) considered these copy events, and their focus was mainly on the discovery of deletions, insertions, and inversions. A more recent algorithm, HYDRA, includes simple heuristics to detect transposon insertions (Quinlan *et al.*, 2010). Interestingly, even if the goal of a method is to identify only insertions, deletions and inversions in a sequenced genome, the presence of the common copy events will cause many false negative deletion and inversion predictions. Figure 1 clearly demonstrates a common scenario where a copy event is mistakenly identified as a large deletion.

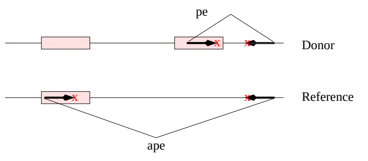

(a) The presence of a copy event in the donor genome and the supporting discordant paired-end mapping.

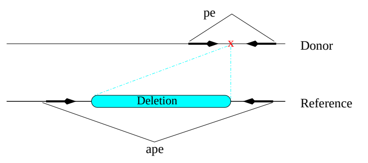

(b) The same discordant mapping as above, however, suggests a large deletion if the annotated repeat element is not considered.

Fig. 1. Transposon insertion causing a false negative deletion prediction. A discordant paired-end read alignment due to a copy event shows identical pattern with a discordant paired-end read alignment supporting a deletion event.

In what follows, we study two classes of copy events and present the set of conditions based on the map locations and orientations of the paired-end alignments that imply a copy event within each of these classes. First, we consider those copy events in which the transposed segment is in direct orientation, and present the set of conditions for all of the four different cases of this class (denoted as Class I). Next, we study the cases for Class II, where the transposon is copied in inverted orientation.

A copy SV of Class I is defined as $SV_{Copy}(Pos_L, Pos_R, Pos_{Br})$, where the genomic segment from positions Pos_L to Pos_R is copied into location Pos_{Br}. Similarly, a copy event $SV_{\overline{Copy}}$ denotes a copy event in inverted orientation.

One of the following four cases should hold for a paired-end read alignment ape that supports a copy event SV_{Copy} (Class I):

Case 1 ($Pos_{Br} < Pos_L$ **and** $or(ape) = +-$) **:**
$\Delta_{\min} < Pos_{Br} - L_r(ape) + R_\ell(ape) - Pos_L < \Delta_{\max}$
(Figure 2(a))

Case 2 ($Pos_{Br} < Pos_L$ **and** $or(ape) = -+$) **:**
$\Delta_{\min} < L_\ell(ape) - Pos_{Br} - R_r(ape) + Pos_R < \Delta_{\max}$
(Figure 2(b))

Case 3 ($Pos_{Br} > Pos_R$ **and** $or(ape) = +-$) **:**
$\Delta_{\min} < R_\ell(ape) - Pos_{Br} + Pos_R - L_\ell(ape) < \Delta_{\max}$
(Figure 2(c))

Case 4 ($Pos_{Br} > Pos_R$ **and** $or(ape) = -+$) **:**
$\Delta_{\min} < Pos_{Br} - R_r(ape) + L_\ell(ape) - Pos_L < \Delta_{\max}$
(Figure 2(d))

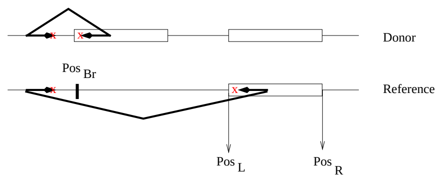

(a) Case 1:$Pos_{Br} < Pos_L$ and $or(ape) = +-$

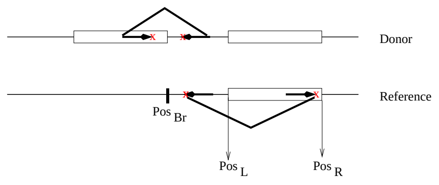

(b) Case 2:$Pos_{Br} < Pos_L$ and $or(ape) = -+$

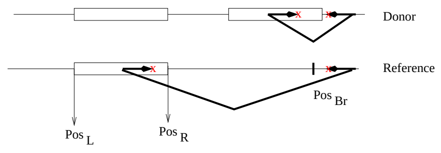

(c) Case 3:$Pos_{Br} > Pos_R$ and $or(ape) = +-$

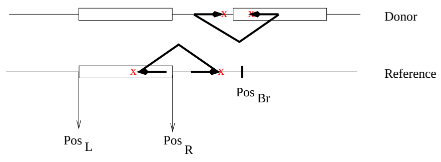

(d) Case 4:$Pos_{Br} > Pos_R$ and $or(ape) = -+$

Fig. 2. The set of conditions for each case that suggests a copy event in which the transposed segment is copied in direct orientation (Class I).

Similarly, one of the following cases should hold for a copy event of Class II:

Case 1 ($Pos_{Br} < Pos_R$ **and** $or(ape) = ++$) **:**
$\Delta_{\min} < Pos_{Br} - L_r(ape) + Pos_R - R_r(ape) < \Delta_{\max}$
(Figure 3(a))

Case 2 ($Pos_{Br} < Pos_R$ **and** $or(ape) = --$) **:**
$\Delta_{\min} < L_\ell(ape) - Pos_{Br} + R_\ell(ape) - Pos_L < \Delta_{\max}$
(Figure 3(b))

Case 3 ($Pos_{Br} > Pos_R$ **and** $or(ape) = ++$) **:**
$\Delta_{\min} < Pos_{Br} - R_r(ape) + Pos_R - L_r(ape) < \Delta_{\max}$
(Figure 3(c))

Case 4 ($Pos_{Br} > Pos_R$ and $or(ape) = --$) :
$\Delta_{\min} < R_\ell(ape) - Pos_{Br} + L_\ell(ape) - Pos_L < \Delta_{\max}$
(Figure 3(d))

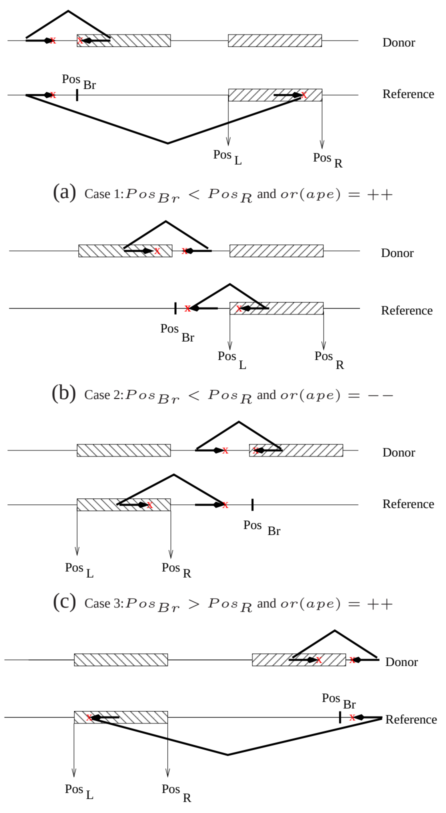

(a) Case 1:$Pos_{Br} < Pos_R$ and $or(ape) = ++$

(b) Case 2:$Pos_{Br} < Pos_R$ and $or(ape) = --$

(c) Case 3:$Pos_{Br} > Pos_R$ and $or(ape) = ++$

(d) Case 4:$Pos_{Br} > Pos_R$ and $or(ape) = --$

Fig. 3. The set of conditions for each case that suggests a copy event in which the transposed segment is copied in inverted orientation (Class II).

3 MAXIMAL VALID CLUSTERS AND COPY EVENT DETECTION

A set of discordant paired-end read alignments that support the same potential SV event is called a "valid cluster" and denoted by $VClu_i = \{a_{i'_1}pe_{i_1}, a_{i'_2}pe_{i_2}, \cdots, a_{i'_\ell}pe_{i_\ell}\}$.

As per (Hormozdiari *et al.*, 2009), a "maximal valid cluster" is defined as a valid cluster where no additional paired-end read alignments can be added such that the cluster remains valid. Note that all paired-end read alignments in maximal valid clusters suggest the same potential structural variation. It was shown that it is sufficient to calculate all maximal valid clusters to solve the maximum parsimony structural variation (MPSV) problem. This can be done in polynomial time (with respect to the number of paired-end alignments), where the computation of *all* valid clusters is unnecessary, and exponential in run time. In (Hormozdiari *et al.*, 2009; Sindi *et al.*, 2009), efficient algorithms to find the maximal valid clusters are presented to predict insertion, deletion, and inversion events.

To find all maximal valid clusters for copy events, a naïve method would investigate all $O(n^3)$ possibilities of potential copy events, for each of the locations Pos_{Br}, Pos_L, and Pos_R between 1 an n, where n is the genome length. This can be done by first creating a cluster for each possible values of Pos_{Br}, Pos_L, Pos_R, and then adding those paired-end reads that satisfy the conditions given in Section 2 to the appropriate cluster. Finally, a set of maximal clusters would be selected. The above method guarantees to find all the maximal valid clusters but it would be time consuming in practice. In what follows, we will present a more efficient method to find all the maximal valid clusters provided that the potential positions of copied segments or copied sequences are known.

We define $\Phi = \{(\phi_{1_\ell}, \phi_{1_r}), (\phi_{2_\ell}, \phi_{2_r}), \cdots, (\phi_{t_\ell}, \phi_{t_r})\}$ as the set of (non-overlapping) segments that can be copied to other locations (Φ can represent the annotated transposons in the reference genome assembly). Note that $\forall\ i \le t$, ϕ_{i_ℓ} is the start location of the i-th segment and ϕ_{i_r} is the end location. The coordinates for the intervals are referred to as "end-points" in the rest of the paper for simplicity.

For each paired-end read mapping ape with exactly one end-read mapped to a transposon (e.g. $\phi_i = (\phi_{i_\ell}, \phi_{i_r})$), there exists a range of locations, or "breakpoint intervals" $Br^i_{ape} = [Br_L, Br_R]$, where ape supports a copy of subsequence $\phi_i = (\phi_{i_\ell}, \phi_{i_r})$ to any location within Br^i_{ape} in the reference genome. Note that for a given ape and a segment $\phi_i = (\phi_{i_\ell}, \phi_{i_r})$, the breakpoint interval Br^i_{ape} can easily be computed using the set of conditions given in Section 2.

Now we present an efficient algorithm [4] to find the maximal valid clusters supporting copy of segment $\phi_i = (\phi_{i_\ell}, \phi_{i_r})$ to any location in genome (the algorithm can trivially be extended for other segments in Φ).

Without loss of generality we assume that there are total of m_i discordant mappings with exactly one end mapped to ϕ_i (Please note that $m = \sum_{i=1}^{t} m_i$, where total number of segments is t). We denote the set of such discordant paired-end read mappings as $ape^i = \{ape^i_1, ape^i_2, \cdots, ape^i_{m_i}\}$. In addition the set of breakpoint intervals for the paired-end read alignments in set ape^i is denoted as $Br^i = \{(Br^i_{1_L}, Br^i_{1_R}), (Br^i_{2_L}, Br^i_{2_R}), \cdots, (Br^i_{m_{iL}}, Br^i_{m_{iR}})\}$.

It is trivial to see that finding maximal valid clusters for all copies of segment $\phi_i = (\phi_{i_\ell}, \phi_{i_r})$ into any position in the genome is equivalent to finding all maximal intersecting breakpoint intervals for all paired-end read mappings ape^i. Thus, we are interested in finding *all maximal intersections* of the breakpoint intervals Br^i.

In what follows, we present an $O(m_i \log m_i + s_i)$ algorithm that outputs all the maximal intersecting intervals (of Br^i), where s_i is the size of the output. This algorithm is the optimal solution to the problem. Please note that an algorithm which finds maximal valid clusters supporting copy of a given segment ϕ_i with running time of $O(m_i \log m_i + s_i)$ will yield an $O(m \log m + S)$ algorithm for finding maximal valid clusters for all the segments in Φ when $S = \sum_{i=1}^{t} s_i$ (since $m = \sum_{i=1}^{t} m_i$).

3.1 Algorithm for finding all maximal intersecting intervals

Given a set of intevals (with cardinality of m_i), we want to find all the maximal intersecting intervals. We first sort all end-points of m_i intervals ($2m_i$ coordinates) in ascending order based on their values.

[4] In fact the algorithm is optimal with respect to the running time.

We call this sorted list of intervals L where each interval appears twice in the list L. We then scan the sorted list from left to right:

- If we observe a point that is at the left end-point of an interval, we insert the interval to a minimum heap data structure, denoted as $heap$. The priority value of the $heap$ is the right end-point of the inserted interval. After each insertion of a new interval to $heap$, we set a flag $newIns = true$.
- If we observe a point that is at the right end-point of an interval, we first check the flag $newIns$. If it is set to *true*, we output all the elements in the $heap$ as one maximal cluster and set $newIns = false$. We then remove the interval from $heap$ since it is guaranteed that the value of the right end-point of the interval removed from the heap is the same as the right end-point of the interval reached in scanned list L. We continue removing intervals from $heap$ until the priority value of the head element of the heap remains unchanged.

The above algorithm outputs all maximal intersecting intervals that are equivalent to the maximal valid clusters.

Complexity : It can be shown that the running time of the above algorithm is $O(m_i \log m_i + s)$, where s is the size of the output. The sorting procedure in the first step of the algorithm takes $O(m_i \log m_i)$. In the worst case, since each removal/insertion operation in the heap takes $O(\log m_i)$ time, the total run time for the second step is also $O(m_i \log m_i)$. It takes $O(s)$ time to write the output. In addition it was previously proven that finding the maximum clique in an interval graph has a lower bound of $\Omega(m_i \log m_i)$ (Gupta *et al.*, 1982). Thus, our algorithm gives the optimal solution for finding all maximal clusters.

3.2 Detection of transposon insertion events from maximal valid clusters

Each maximal valid cluster for different SV types (i.e. insertion, inversion, deletion or copy) only suggests a *potential* structural variation. The fact that each paired-end read can be mapped to multiple locations that are included in multiple maximal valid clusters proves that some of these implied potential variants are incorrect. We previously presented a combinatorial method to select the minimum number of these clusters (equivalent to selecting minimum number of structural variants), such that each paired-end read has a map location in at most one selected valid cluster (Hormozdiari *et al.*, 2009). This problem was called Maximum Parsimony Structural Variation (MPSV), and an approximation algorithm was given. The same algorithm presented can be used to find transposon insertion events from the maximal valid clusters using the algorithms presented in the previous section.

In the next section, we introduce an extension to Maximum Parsimony Structural Variation problem, and provide an efficient method to solve it. We show that our new method outperforms our previous algorithm in (Hormozdiari *et al.*, 2009).

4 MAXIMUM PARSIMONY STRUCTURAL VARIATION WITH CONFLICT RESOLUTION

As mentioned before, the possibility of multiple map locations for each paired-end read raises the question of resolving which structural variants implied by the maximal valid clusters are *correct*.

The Maximum Parsimony Structural Variation (MPSV) problem (Hormozdiari *et al.*, 2009) aims to compute a unique mapping for each discordant paired-end read in the reference genome such that the total number of implied SV is minimized (in this section we consider all classes of SV). In (Hormozdiari *et al.*, 2009), MPSV was modeled as a combinatorial optimization problem and shown to be NP-complete. An approximation algorithm (denoted as VariationHunter) based on the *set-cover* problem with $O(\log n)$ approximation factor was given. However, the modeling of the MPSV problem imposed no limits on the number of “overlapping” SV predictions. A considerable amount of the predicated calls overlap with each other and a post-processing heuristic to filter some of those overlapping predicted SVs was given (see the Results section of (Hormozdiari *et al.*, 2009)). In this section we mathematically formulate these “conflicts” and model the structural variation discovery problem as a *novel* combinatorial optimization problem.

4.1 Conflicting SV clusters in haploid and diploid genome sequences

We motivate the “conflict resolution” for structural variation using a simple example. Given paired-end reads from a *haploid* genome, a structural variation detection algorithm (such as VariationHunter, MoDIL or BreakDancer) might construct two or more sets of valid clusters that imply multiple conflicting deletion calls (Figure 4). Assuming the genome is haploid, it is not possible that both valid clusters in Figure 4 can be “correct”.

We first formalize the Maximum Parsimony Structural Variation with Conflict Resolution (MPSV-CR) for both haploid and diploid genomes, and then we analyze the complexity of the MPSV-CR problem. Finally, we provide a heuristic solution for MPSV-CR. We call this solution as VariationHunter with Conflict Resolution (VariationHunter-CR).

Assuming a haploid genome, two valid clusters $Vclu_1$ and $Vclu_2$ of paired-end reads are *conflicting* if and only if there exists a potential scenario of structural variants implied by the two valid clusters, such that the existence of one of the events makes the other valid cluster incoherent (Figure 4). In the Supplementary Material, we present the set of rules to determine whether two valid clusters are in conflict in a haploid genome.

Through the conflict rules we can model the conflict representation of all clusters using a graph denoted as *conflict graph*. Each cluster is represented a node, and there exists an edge between two nodes if and only if the two corresponding clusters are in conflict with each other. It is not difficult to see that a valid set of SVs is a set of nodes/clusters in which no two nodes within the subset are connected. In another words, the valid solution (without any conflicts) is an independent set of the conflict graph.

One can easily generalize the definition of conflicting clusters to *diploid* genome sequences. Let $Vclu_1$ and $Vclu_2$ be two conflicting clusters in a haploid genome. However, provided that the genome is diploid, both $Vclu_1$ and $Vclu_2$ might imply a correct SV in different haplotypes. Now consider a third SV cluster, $Vclu_3$ that is in conflict with both $Vclu_1$ and $Vclu_2$. It is trivial that, based on the pigeon hole principle, $Vclu_1$, $Vclu_2$, and $Vclu_3$ cannot simultaneously occur in a diploid genome. In other words, the presence of three different SV clusters that are conflicting pairwise in a haploid genome [5] will be a conflict in a diploid genome. The concept of the conflict graphs for haploid genomes can be replaced with *conflict hypergraphs* for diploid

[5] According to our definition of conflicts in a haploid genomes.

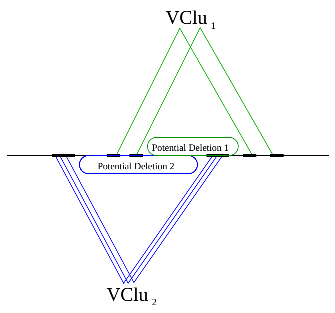

Fig. 4. Two valid clusters $Vclu_1$ and $Vclu_2$ are shown to be in conflict in a haploid genome.

genomes. In the conflict hypergraph each hyperedge connects three nodes, if these three nodes are in conflict with each other.

Now, we define the Maximum Parsimony Structural Variation with Conflict Resolution (MPSV-CR) problem that does not only aim to minimize the total number of implied structural variants but also guarantees that no pairwise conflicting triplet of the implied SVs exists.

Note that this new version of the MPSV problem does not select any conflicting structural variants and thus may not always be able to assign every paired-end read to a particular SV. Thus the optimization function for MPSV-CR not only tries to minimize the number of SVs predicted, but also maximizes the number of paired-ends that can be assigned to a location in genome.

In what follows we present the concept of conflicting SV clusters in more detail and give a formal definition of the MPSV-CR problem.

4.2 Formal definition of the MPSV-CR problem

In this section, we formally define the MPSV-CR problem. Let $MC = \{VClu_1, VClu_2, \cdots, VClu_n\}$ be the set of SV clusters and $R = \{pe_1, pe_2, \cdots, pe_m\}$ be the collection of discordant paired-end reads. These discordant read pairs can be mapped to multiple locations in the genome, represented by $Align(pe_i) = \{a_1pe_i, a_2pe_i, \cdots, a_jpe_i\}$.

In order to formulate the constraints, we define the conflict hypergraph CG as a hypergraph with vertex set $V(CG) = MC$ and a hyperedge set $E(CG)$ as follows. Between every *three* distinct SV clusters that are pairwise in conflict, there exists a hyperedge in $E(CG)$:

$$E(CG) = \{(VClu_i, VClu_j, VClu_k) \mid VClu_i, VClu_j, VClu_k \text{ are pairwise in conflict}\}$$

Note that for the case when we only deal with a haploid genome (rather than a diploid genome), the hypergraph is nothing else than a simple graph (denoted by G) where each $e \in E(G)$ represents a pair of conflicting SV cluster.

A subset $SC \subset MC$ is *satisfiable* under the constraint hypergraph CG, if $\nexists e = (VClu_p, VClu_q, VClu_r) \in E(CG) : e \subseteq SC$ (in the case of a haploid genome a subset $SC \subset MC$ *satisfiable* under the constraint graph G, if $\nexists e = (VClu_p, VClu_q) \in E(G) : e \subseteq SC$).

For each satisfiable subset SC and each paired-end read pe_i, we define the indicator variable $\delta(SC, pe_i)$ as follows:

$$\delta(SC, pe_i) = \begin{cases} 0 & \text{if } \exists SC_k \in SC \bigwedge \exists j : a_jpe_i \in SC_k \\ 1 & \text{otherwise} \end{cases}$$

Intuitively, $\delta(SC, pe_i)$ is the penalty for not assigning the pair-end read pe_i to a cluster in the satisfiable subset SC. The MPSV-CR problem aims to find the satisfiable set SC' such that $f(SC') = |SC'| + \sum_{pe \in R} \delta(SC', pe)$ is *minimized* (i.e. to find a trade-off between the number of SV clusters in a satisfiable set and the number of paired-end reads that are not assigned to any SV clusters.).

Computational complexity of MPSV-CR: Here we prove that MPSV-CR is NP-hard, independent from the weights on the cardinality of SC' and the penalty for unmapped reads (i.e. minimizing the function $g(SC') = k \cdot |SC'| + l \cdot \sum_{pe \in R} \delta(SC', pe)$ for any $k > 0$ and $l > 0$ is NP-hard). The NP-hardness proof follows a reduction from the minimum set cover problem (See the Supplementary Materials for the detailed proof). In addition, we show an inapproximability result for MPSV-CR problem even when the genome is assumed to be haploid.

THEOREM 4.1. *There is no constant $\epsilon > 0$ for which MPSV-CR on haploid genome can be approximated within a factor of $n^{1-\epsilon}$ in polynomial time, unless $P = NP$.*

Proof of Theorem 4.1 given in the Supplementary Material.

4.3 An efficient solution to the MPSV-CR problem

In this section we present a heuristic solution for a special case of the MPSV-CR problem where both k and l (the coefficients in the optimization function g) are set as $k = 1, l = 1$. This heuristic, named as $Max\_Assigned\_Reads$, consists of two phases:

In the first phase, we form a *maximal satisfiable set* of SV clusters (denoted by MS) in a greedy fashion. Note that a satisfiable set of SV clusters, SC (as noted in the previous section), is called *maximal* if no other SV cluster $VClu$ can be added to SC such that $VClu$ together with two existing SV clusters in SC form a hyperedge in the conflict hypergraph CG. We start with $MS = \emptyset$ and then iteratively add the SV cluster that covers the most number of paired-end reads [6] to MS until MS becomes a maximal satisfiable set. Note that we add an SV cluster SV_k to MS in an iteration even if SV_k does not cover any *new* discordant paired-end read (provided that MS remains satisfiable). We denote MR as the set of all paired-end reads covered by the SV clusters in MS.

In the second phase of $Max\_Assigned\_Reads$, the aim is to select the minimum number of SV clusters from MS that cover all paired-end reads in MR. For this phase we use a set cover approach similar to Hormozdiari *et al.* (2009).

In what follows, we give a lower bound on the cardinality of MR. The analysis of the second phase of $Max\_Assigned\_Reads$ is similar to Hormozdiari *et al.* (2009). Let m be the total number of discordant paired-end reads, and let $neighbors(VClu) = \{VClu' | \exists e \in E(CG), VClu, VClu' \in e\}$, $deg(VClu) = |neighbors(VClu)|$ and $\Delta = \max\{deg(VClu) | VClu \in MC\}$ i.e. the maximum degree of a vertex in the conflict graph CG.

THEOREM 4.2. $|MR| \geq m/(\Delta + 1)$.

PROOF. Let k be number of iterations of $Max\_Assigned\_Reads$. For each i ($1 \leq i \leq k$), we denote $VClu_i$ as the cluster that is selected at the i^{th} iteration. We also denote MR_i as the set of paired-end reads that are covered by $VClu_i$ for the first time. Furthermore, we define UR_i as the set of paired-end reads that are not covered by any of the SV clusters $VClu_1$ through $VClu_i$ and also is not able to be covered later (as the result of selecting $VClu_i$) in the remaining $k-i$ iterations.

At the i^{th} iteration, the maximum number of reads that could be covered for all neighbors of $VClu_i$ is at most $\Delta|MR_i|$, thus

[6] We count the paired-end reads that were not previously covered by any SVs in MS

$|UR_i| \leq \Delta|MR_i|$. Moreover, we have $\sum_{i=1}^{k}(UR_i + MR_i) = m$ and $|MR| = \sum_{i=1}^{k} MR_i$. Hence $m/(\Delta+1) \leq |MR|$.

5 EXPERIMENTAL RESULTS

5.1 Implementation

It is established that there are a large number of mobile elements in the human genome (Mills *et al.*, 2007). For example, the reference human genome assembly annotation includes 1 million copies of the Alu element. Considering all known mobile elements (segments in genome) as potential transposon sequences for our algorithm would be very time consuming, and in fact, unnecessary. The consensus sequences for all mobile elements are well studied, and available at the RepBase database (Jurka *et al*., 2005). We used the consensus sequences of these mobile element families as representative sequences to facilitate faster experimentation. To this end, we create a new sequence, denoted as chrN: we first append a poly-N sequence to each consensus sequence, and then concatenated them, generating chrN. In this paper, we considered only Alu and SVA elements in our experiments.

For read mapping we use mrsFAST (Hach *et al*., 2010), a cache-oblivious short read mapper recently developed as an extension of mrFAST (Alkan *et al*., 2009). mrsFAST maps the paired-end reads to *all* locations with Hamming distance less than a user-defined threshold ω. In this experiment we set $\omega = 2$.

Given paired-end whole-genome shotgun sequence library $R = \{pe_1, pe_2, \cdots pe_n\}$, we follow the following steps to obtain the reads (and mapping information) for transposon discovery:

- We first map all paired-end reads to chrN using mrsFAST and discard such paired-end reads that cannot be mapped to chrN. We keep the read pairs where one end-read is mapped to chrN.
- Next, we map the reads we determine in the previous step to the reference genome, and discard all paired end reads with at least one *concordant* mapping.
- Finally we re-map the reads from Step 2 to both chrN and the reference genome. As a post-processing step, we select the paired-end alignments where one end is mapped to chrN and the other end is mapped to the reference genome.

5.2 Mobile element insertion discovery in the Venter genome

A list of mobile element insertions in the Venter genome assembly (HuRef) (Levy *et al*., 2007) in comparison to reference human genome assembly (NCBI build 36) genome was recently published (Xing *et al*., 2009). We used the available HuRef genome to produce short paired-end reads, similar to reads generated by the Illumina technology (simulating an Illumina sequencing of the Venter genome) to benchmark the sensitivity and specificity of our algorithms. To our knowledge this is the only dataset for mobile element insertion annotations from the genome of a single individual. We created paired-end reads from the HuRef genome with a read length of 36 bp, and obtained 10-fold sequence coverage. The fragment insert sizes for paired-end reads were chosen randomly that follows a normal distribution very similar to the fragment size distribution in the NA18507 shotgun sequence library generated using the Illumina platform (Bentley *et al*., 2008)).

We used our mobile element insertion discovery algorithm to discover transposons in the autosomes of HuRef (from chr1 to chr22). In our experiments, we focused on Alu, NCAI (Non-classical Alu Insertion)[7], and SVA insertions. The results of our experiment are summarized in Table 1. The validated set of mobile element insertions in the HuRef assembly is a union of the published transposon insertions in (Xing *et al*., 2009) and our *new* transposon predictions not listed in (Xing *et al*., 2009) but are included in HuRef.

As shown in Table 1, our method was able to find most of the known/validated mobile element insertions (recall rate is $> 85\%$) while the number of invalidated predictions is very low (precision rate $\sim 90\%$).

Interestingly, most of the Alu insertions missed by our algorithm were truncated insertions (significantly smaller than the consensus sequences). Figure 5 summarizes the true positive / false negative results with respect to the length of Alu insertion.

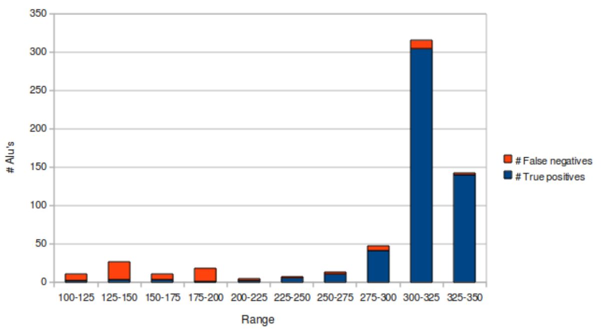

Fig. 5. The length distribution of true positive and false negative mobile element insertion predictions for Alu elements. Note that all of the Alu consensus sequences used in creating chrN are longer than 250 bp.

5.3 Structural Variation Prediction with VariationHunter-CR

In this section we show that the call set predicted by VariationHunter with conflict resolution (VariationHunter-CR) has a lower false positive rate than the original VariationHunter (Hormozdiari *et al*., 2009) while retaining the same true

[7] Alu insertions that only contain the internal fragment of Alu are called Non-classical Alu insertions (NCAI) (Xing *et al*., 2009).

Table 1. Summary of mobile element insertion prediction results in the Venter genome. We show the precision and recall rates of our mobile element (Alu, NCAI, and SVA) insertion discovery. We compare our mobile element insertion predictions with both (Xing *et al.*, 2009) and the HuRef genome assembly(Levy *et al.*, 2007). The results demonstrate that our algorithm has a high recall and precision rate.

Chromosome	Validated	Predicted	Found	Recall	Precision
Chromosome 1	41 Alu 4 NCAI	42 Alu	40	88%	95%
Chromosome 2	59 Alu 2 NCAI	57 Alu	56	91%	98%
Chromosome 3	42 Alu 1 NCAI 1 SVA	40 Alu	40	90%	100%
Chromosome 4	43 Alu 4 NCAI	41 Alu 1 NCAI	40 1	87%	97%
Chromosome 5	39 Alu 1 SVA	44 Alu 1 SVA	35 1	90%	80%
Chromosome 6	59 Alu 1 NCAI 1 SVA	55 Alu 1 SVA	53 1	88%	96%
Chromosome 7	24 Alu	22 Alu	20	83%	91%
Chromosome 8	34 Alu 2 NCAI	33 Alu	33	92%	100%
Chromosome 9	23 Alu 1 NCAI 1 SVA	23 Alu 1 NCAI	21 1	88%	92%
Chromosome 10	33 Alu 2 NCAI	32 Alu 1 NCAI	32 1	94%	100%
Chromosome 11	35 Alu 3 NCAI 2 SVA	32 Alu 1 NCAI 1 SVA	32 1 1	85%	100%
Chromosome 12	33 Alu 4 NCAI	34 Alu	31	84%	91%
Chromosome 13	34 Alu 3 NCAI 2 SVA	34 Alu 1 SVA	34 1	90%	100%
Chromosome 14	19 Alu 1 NCAI 2 SVA	20 Alu 2 SVA	19 2	95%	95%
Chromosome 15	24 Alu	21 Alu	20	83%	95%
Chromosome 16	12 Alu 3 NCAI	12 Alu 1 NCAI	12 1	80%	100%
Chromosome 17	9 Alu 2 NCAI 2 SVA	9 Alu 1 SVA	9 1	77%	100%
Chromosome 18	22 Alu	21 Alu	20	91%	95%
Chromosome 19	11 Alu 3 NCAI 1 SVA	11 Alu 1 NCAI	11 1	80%	100%
Chromosome 20	11 Alu 2 NCAI	13 Alu 1 NCAI	9 1	77%	71%
Chromosome 21	7 Alu	7 Alu	7	100%	100%
Chromosome 22	7 Alu	5 Alu	5	71%	100%

positive rate (Supplementary Material includes simulations supporting this claim). As an experiment we compare the deletion predictions using different algorithms including VariationHunter-CR in the genome of a Yoruba African donor (NA18507) sequenced with the Illumina Genome Analyzer platform (Bentley *et al.*, 2008). We include the validated deletions detected in the genome of the same individual using fosmid clone-end sequencing (Kidd *et al.*, 2008) in our comparisons.

We downloaded approximately 3.5 billion end-sequences ($\sim$ 1.7 billion pairs) of length $36 - 41$ bp and insert size $\sim$ 200 bp from the NCBI Short Read Archive[8]. Similar to the pre-screening methodology used in (Hormozdiari *et al.*, 2009), we removed any pairs of reads from consideration if either (or both) end-sequences has average *phred* (Ewing and Green, 1998) quality score less than 20, or if either (or both) sequences contain more than 2 N characters. In total, $\sim$ 1.3 billion reads were removed from this data set. We then mapped all the remaining $\sim$ 2.2 billion end sequences to the human reference genome using *mrFAST* (Alkan *et al.*, 2009). The average insert size was determined to be 209 bp, where the standard deviation was 13.4 bp.

Figure 6 shows the comparison of our new VariationHunter-CR algorithm with the original VariationHunter, the curated (post-processed to remove conflicting predictions) result published in (Hormozdiari *et al.*, 2009) and BreakDancer (Chen *et al.*, 2009).

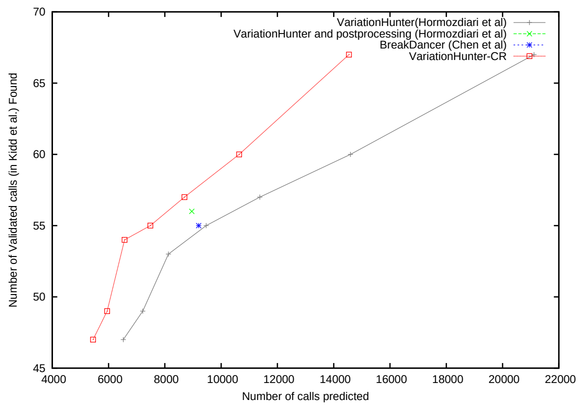

Fig. 6. Prediction performance comparisons of VariationHunter (black), VariationHunter-CR (red) and BreakDancer (blue). We also show the curated (post-processed) results of VariationHunter in this figure (green). The x-axis represents the number of deletions predicted by each method, and y-axis is the number of validated deletions from (Kidd *et al.*, 2008) that overlaps ($> 50\%$ reciprocal overlap) with a prediction. It is desirable to obtain a prediction set is able to find more validated calls with less number of total calls For VariationHunter and VariationHunter-CR we give the number of calls and number of validated deletions found for different support levels (number of paired-end read supporting them); less support level results in more predicted deletion intervals. This figure shows that VariationHunter-CR has a better performance than VariationHunter for all support levels, and both VariationHunter and VariationHunter-CR outperform the BreakDancer algorithm (Chen *et al.*, 2009).

6 CONCLUSION

Despite recent advances in algorithm design for the detection of structural variation, due to the difficulty in discovering complex variants in regions of the genome with high plasticity the existing algorithms are still at their infancy. In this paper, we presented the "Next-Generation" of our structural variation discovery algorithm VariationHunter that aims to improve both the sensitivity and specificity of SV detection. VariationHunter is now capable of resolving incompatible

[8] ftp://ftp.ncbi.nih.gov/pub/TraceDB/ShortRead/SRA000271

SV calls through a conflict resolution mechanism that no longer requires post-processing heuristics. Furthermore, we described additional algorithms to discover mobile element insertions that are of know importance to genome evolution and genomic variation. These enhancements provide a much needed step towards a highly reliable and comprehensive structural variation discovery algorithm, which, in turn will enable genomics researchers to better understand the variations in the genomes of newly sequenced human individuals, as well as the genome structures of non-human species.

ACKNOWLEDGMENTS

We would like to thank T. Brown, L. Brunner and H. Yaghoubi for their help in manuscript preparation. This work was supported, in part, by Natural Sciences and Engineering Research Council of Canada (NSERC) and Genome BC grants to S.C.S, and U.S. National Institutes of Health grant HG004120 to E.E.E. E.E.E. is an investigator of the Howard Hughes Medical Institute.

REFERENCES

Alkan C., et al. (2009) Personalized copy number and segmental duplication maps using next-generation sequencing, *Nature Genetics*, **41**, 1061–1067.

Bailey J.A., et al. (2003) An Alu transposition model for the origin and expansion of human segmental duplications, *Am J Hum Genet*, **73**, 823–34.

Bashir A., et al. (2008) Evaluation of paired-end sequencing strategies for detection of genome rearrangements in cancer, *PLoS Comput Biol*, **4**, e1000051.

Bekpen C., et al. (2009) Death and resurrection of the human IRGM gene, *PLoS Genet*, **5**, e1000403.

Bentley D.R., et al. (2008) Accurate whole human genome sequencing using reversible terminator chemistry, *Nature*, **456**, 53–59.

Chen K., et al. (2009) Breakdancer: an algorithm for high-resolution mapping of genomic structural variation, *Nature Methods*, **6**, 677–681.

Du J.,et al. (2009) Integrating sequencing technologies in personal genomics: optimal low cost reconstruction of structural variants, *PLoS Comput Biol*, **5**, e1000432.

Ewing B., Green P. (1998) Base-calling of automated sequencer traces using phred. II. error probabilities, *Genome Res*, **8**, 186–94.

Feuk L., et al. (2006) Structural variation in the human genome, *Nat Rev Genet*, **7**, 85–97.

Gupta U.I., et al. (1982) Efficient algorithms for interval graphs and circular-arc graphs, *Networks*, **12**, 459–467.

Hach F., et al. (2010) Cache oblivious algorithms for high throughput read mapping, *unpublished*.

Hancks D.C., et al. (2009) Exon-trapping mediated by the human retrotransposon SVA, *Genome Res*, **19**, 1983–1991.

Hollox E., et al. (2008) Psoriasis is associated with increased bold beta-defensin genomic copy number, *Nature Genetics*, **40**, 23–25.

Hormozdiari F., et al. (2009) Combinatorial algorithms for structural variation detection in high-throughput sequenced genomes, *Recomb 2009/Genome Research*, **19**, 1270–1278.

Jurka J., et al. (2005) Repbase update, a database of eukaryotic repetitive elements, *Cytogenet Genome Res*, **110**, 462–467.

Kidd J.M., et al. (2008) Mapping and sequencing of structural variation from eight human genomes, *Nature*, **453**, 56–64.

Korbel J.O., et al. (2009) PEMer: a computational framework with simulation-based error models for inferring genomic structural variants from massive paired-end sequencing data, *Genome Biol*, **10**, R23.

Korbel J.O., et al. (2007) Paired-end mapping reveals extensive structural variation in the human genome, *Science*, **318**, 420–426.

Lee S., et al. (2008) A robust framework for detecting structural variations in a genome, *Bioinformatics*, **24**, i59–i67.

Lee S., et al. (2009) Modil: detecting small indels from clone-end sequencing with mixtures of distributions, *Nature Methods*, **6**, 473 – 474.

McCarroll S.A., et al. (2008) Deletion polymorphism upstream of IRGM associated with altered IRGM expression and Crohn's disease, *Nat Genet.*, **40**, 1107–1112.

Levy S., et al. (2007) The diploid genome sequence of an individual human, *PLoS Biol*, **5**, e254.

Medvedev P., et al. (2009) Computational methods for discovering structural variation with next-generation sequencing, *Nat Methods*, **6,** 13–20.

Mills R.E., et al.(2007) Which transposable elements are active in the human genome?, *Trends Genet*, **23**, 183–191.

Quinlan A.R., et al. (2010) Genome-wide mapping and assembly of structural variant breakpoints in the mouse genome, *Genome Res*, in press.

Sindi S., et al. (2009) A geometric approach for classification and comparison of structural variants, *Bioinformatics*, **25**, i222-i230.

Tuzun E., et al. (2005) Fine-scale structural variation of the human genome, *Nat Genet* **37**, 727–32.

Volik S., et al. (2003) End-sequence profiling: sequence-based analysis of aberrant genomes, *Proc Natl Acad Sci U S A*, **100**, 7696–701.

Xing J., et al. (2009) Mobile elements create structural variation: analysis of a complete human genome, *Genome Res*, **19**, 1516–1526.